Article

Energy Transfer of Electronic Excitations by Activators in Phosphates and Sulfates via the Creation of Combined Electron Emission States

Aibek S. Nurpeissov [1,]*, Temirulan T. Alibay [1], Turlybek Nurakhmetov [1], Aivaras Kareiva [2], Aleksej Zarkov [2] and Sapargali Pazylbek [2]

1 Department of Technical Physics, L.N. Gumilyov Eurasian National University, 2 Satpaeva St, Nur-Sultan ZO1A3D7, Kazakhstan

2 Institute of Chemistry, Faculty of Chemistry and Geosciences, Vilnius University, Naugarduko 24, LT-03225 Vilnius, Lithuania

* Correspondence: lord_sukre@mail.ru

Abstract: In this work, the mechanisms for creating a combined electronic–radiative local state beneath the conduction band, consisting of intrinsic and activator electron–hole states, are experimentally substantiated. In the first part of this work, the mechanisms of the formation of intrinsic and activator electron–hole trapping centers are experimentally demonstrated in all four matrices with activators. Intrinsic electronic states are localized on activators and anions of the matrix, forming intrinsic and activator electronic states. The hole component of the electron–hole pairs is localized near the activators. Thus, the energy of intrinsic electronic excitations localized in the matrix in the form of combined electronic–radiative states is observed at 3.06–3.1 eV and 2.92–2.95 eV. Radiative states are excited by photon energies of ~4.5 eV and ~4.0 eV, resulting in recombination emissions at 3.06–3.1 eV and 2.92–2.95 eV, as well as activator emissions at 2.06 eV for Mn^{2+}, 2.5 eV for Tb^{3+}, and 2.56 eV and 2.16 eV for Dy^{3+}. Energy transfer from the matrix to emitters or activators occurs during the decay of the combined radiative state. Upon heating, electrons localized on anions and activators delocalize at temperatures of 200–350 K. The energy released during the recombination of an electron with a hole near the activators is transferred to the activators. This process facilitates energy transfer to activators in dosimeters and detectors.

Keywords: emission and excitation spectra; electron–hole; phosphates; recombination emissions trapping centers; vacuum ultraviolet

1. Introduction

Emission bands at 2.17 eV, 2.08 eV, and 2.14 eV in $Ca_2P_2O_7 - Mn$ are excited by photons with energies of 2.48 eV, 3.1 eV, 2.95 eV, and 3.44–3.65 eV. According to the authors of [1,2], these excitation bands correspond to the forbidden intracenter transitions of Mn^{2+} ions in the matrix. It has been shown that the 1.93 eV emission is effectively excited by the intracenter transitions of Mn^{2+} ions, as well as by photons with an energy of 5.98 eV, which corresponds to charge transfer from the $Ca_5Mn(PO_4)_7$ matrix to Mn^{2+} activators, $O^{2-}—Mn^{2+}$.

The authors of [3] discovered thermoluminescence in YPO_4 activated with Ce^{3+}, Ln^{3+} $\left(Nd^{3+}, Er^{3+}, Ho^{3+}, Dy^{3+}\right)$ and associated the presence of an electron trapping center, where an electron localization was $Ln^{3+} + e^- \rightarrow Ln^{2+}$, with the formation of electron and hole trapping centers in this matrix.

The formation of trapping centers in pure matrices and phosphors with activators leads to energy transfer from the matrix to the activators.

The authors of [4,5] demonstrated that in the phosphor $Ca_3(PO_4)_2 - Mn$, emission with an energy of 1.97 eV is associated with Mn^{2+} activators and is excited by intracenter transitions of the Mn^{2+} ion, as well as by photons with an energy of 4.96 eV, due to charge transfer from the excited anion PO_4^{3-} (O^{2-}—Mn^{2+}) to Mn^{2+} ions. As a result, activator electron trapping centers $Mn^+ - PO_4^{2-}$ are formed.

The authors of [6–10] suggest that the appearance of a dosimetric TSL peak in irradiated $CaSO_4 - Dy$ phosphors is associated with the decomposition of the SO_4^{2-} anionic complex into radicals SO_4^-, SO_3^-, SO_2^-, and O_3^-. During annealing, such electron–hole trapping centers recombine, resulting in dosimetric TSL peaks.

In studies [11–29], it was experimentally shown that the sensitivity of dosimetric TSL peaks in $CaSO_4 - Dy$ can be increased by introducing various activators, annealing the matrix at high temperatures, etc.

A brief literature review shows that in many phosphates and sulfates, when excited within the fundamental matrix region where free electrons and holes are created, trapping centers form due to the localization of electrons and holes on activators or intrinsic matrix defects.

There are studies where activators or intrinsic trapping centers are created at photon energies insufficient to generate free electron–hole pairs. It is assumed that experimentally observed trapping centers are formed as a result of charge transfer from an excited anion to activators or neighboring anions. The mechanism of the process leading to the formation of electron or hole trapping centers remains unexplained.

In this work, we substantiate the new model of energy transfer from the matrix to activators proposed in our previous studies [30,31]. We hypothesize that energy transfer from the matrix to activators requires the creation of bound electron-radiative states involving both the matrix and activators through the formation of activator and intrinsic trapping centers. These radiative states accumulate the energy of the intrinsic matrix, which must then be transferred to the activators.

In this study, we aim to show that the new energy transfer mechanism from the matrix to activators is fundamental. For comparison, we selected four matrices of phosphates and sulfates with different activators: $Ca_2P_2O_7 - Mn$, $BaSO_4 - Dy$, $Ca_2P_2O_7 - Tb$, and $Ca_3(PO_4)_2 - Mn$.

2. Objects and Methods of Research

The *Mn*-doped $Ca_2P_2O_7$ and $Ca_3(PO_4)_2$ were synthesized using a wet co-precipitation method followed by annealing at 1200 °C. The phosphors were obtained based on a slightly modified version of a previously described procedure [2,32].

In this method, calcium nitrate tetrahydrate (Ca(NO$_3$)$_2$ · 4H$_2$O, Carl Roth, >99%), manganese(II) nitrate tetrahydrate (Mn(NO$_3$)$_2$ · 4H$_2$O, 98%, Alfa Aesar, Haverhill, MA, USA), and diammonium hydrogen phosphate ((NH4)$_2$HPO$_4$, Carl Roth, >98%) served as the starting materials. A 0.8 M solution of Ca^{2+} and Mn^{2+} nitrates was prepared by dissolving the respective metal salts in deionized water, with Mn substitution set at 1 mol% relative to Ca^{2+} ions. A separate solution of (NH$_4$)$_2$HPO$_4$ with the same concentration was prepared independently.

The phosphate solution was quickly added to the metal ion solution under continuous stirring on a magnetic stirrer, which led to the formation of precipitates. These precipitates were aged in the reaction mixture for 5 min while stirring and then filtered, rinsed with deionized water, and dried in an oven at 50 °C for 10–12 h.

The $Ca_3(PO_4)_2 - Mn$ and $Ca_2P_2O_7 - Tb$ samples were synthesized using the same method.

The obtained powders of $Ca_2P_2O_7 - Mn$ and $Ca_3(PO_4)_2 - Mn$ were annealed for 5 h at 1000 °C for synthesis, while the $Ca_2P_2O_7 - Tb$ sample was annealed for 5 h at 1000 °C. For both $Ca_2P_2O_7 - Mn$ and $Ca_3(PO_4)_2 - Mn$ a shorter annealing process was followed at 1200 °C (10 min), while for the $Ca_2P_2O_7 - Tb$ sample the annealing temperature was 1100 °C (10 min) with a heating rate of 5 °C/min to reduce the evaporation of phosphate species. After annealing, the furnace was allowed to cool down naturally.

During the synthesis of $BaSO_4 - Dy$ samples, 99.99% pure barium sulfate (Sigma-Aldrich, St. Louis, MO, USA) and Dy_2O_3 (Sigma-Aldrich) were used following the slow evaporation method. To prepare $BaSO_4$ (0.8 mol%), 5 g of powder was measured, and a calculated amount of Dy_2O_3 activator was added and mixed thoroughly. The activator mass was determined using the following formula:

$$m_1 = m_2 \frac{M_1 n}{M_2(100 - n)}$$

The mixed powder was dissolved in highly concentrated sulfuric acid, washed multiple times with double-distilled water, and subjected to slow evaporation at 60 °C until dry. The resulting material was annealed in an argon atmosphere using an electric furnace (SNOL, 8.2/1100, Lithuania) at 400 °C for 5 h, followed by slow cooling within the furnace.

Tablet-shaped samples were created for measurement purposes by compressing the powder in a hydraulic press under 7–8 MPa [30].

3. Characterization

X-ray powder diffraction (XRD) analysis was conducted using Ni-filtered Cu-Kα radiation on a Rigaku MiniFlex II diffractometer, operating in Bragg–Brentano geometry ($\theta/2\theta$). Data were collected in the angle range of 2θ from 10 to 60°, with a step size of 0.02° and a scanning rate of 1°/min.

The morphology of the synthesized products was studied using a Hitachi SU-70 field emission scanning electron microscope (Tokyo, Japan). Emission and excitation spectra measurements in the spectral range from 6.2 eV to 12.4 eV (100–200 nm) were carried out using a vacuum monochromator assembled according to the Seya–Namioka scheme with a Solar M-266 recording monochromator (Solar LS, Minsk, Belarus) and a Hamamatsu H11890-01 photomultiplier tube detector (Hamamatsu Photonics, Shizuoka Prefecture, Japan). A hydrogen lamp is used for excitation in the VUV range of the spectrum. Cooling to 15 K is provided by a closed-cycle helium cryostat.

For the measurement of emission spectra in the range of 1.5–6.2 eV, a Solar SM 2203 spectrofluorometer (Solar LS, Minsk, Belarus) was used. Low-temperature studies (77 K) utilized a cryostat with a vacuum of 10^{-4} Pa, cooled by liquid nitrogen.

4. Experimental Results

The crystallinity and purity of the synthesized powders were evaluated by X-ray diffraction analysis. The X-ray diffractograms of the $Ca_2P_2O_7$ (a) sample doped with Mn and $Ca_2P_2 - Tb$ (c) after annealing are shown in Figure 1. The diffraction peaks correspond to the standard pattern for $Ca_2P_2O_7$ (PDF #073-0440) and for the $Ca_2P_2 - Tb$ sample (PDF #00-009-0345), confirming the successful formation of the target material.

X-ray structural analysis of $Ca_3(PO_4)_2 - Mn$ and $BaSO_4 - Dy$ samples was conducted at room temperature. The results of the XRD study are shown in Figure 1b,d. According to the measurement results, the $Ca_3(PO_4)_2 - Mn$ samples correspond to the standard card

(PDF #96-151-7239), and for $BaSO_4 - Dy$, a similarity was found with the standard (PDF #96-100-0038), with no uncontrolled activators detected.
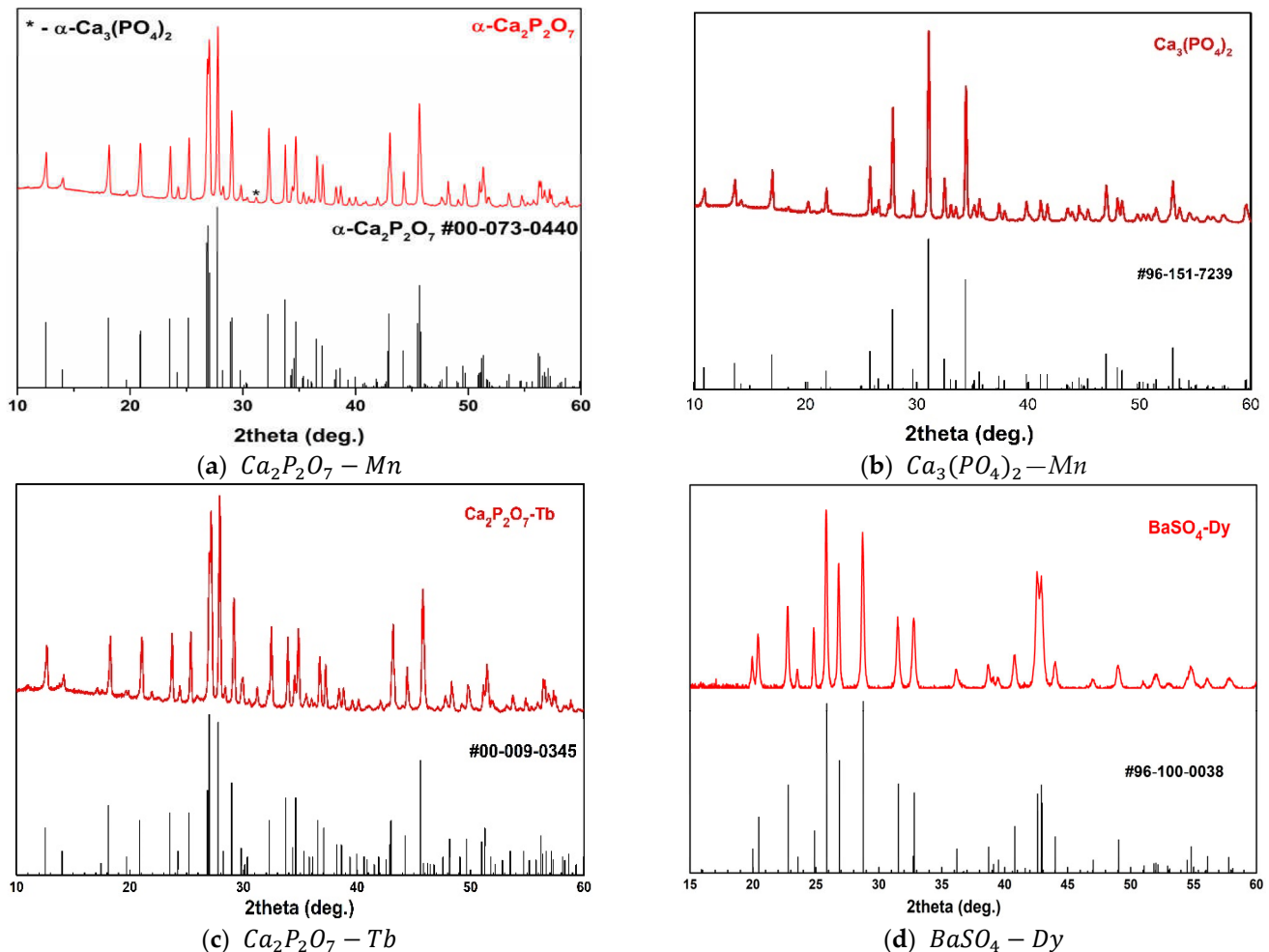

Figure 1. XRD spectra of the samples.

Figure 2 presents the emission spectra of $Ca_2P_2O_7 - Mn$ (a) [31], $Ca_3(PO_4)_2 - Mn$ (b), $Ca_2P_2O_7 - Tb$ (c) and $BaSO_4 - Dy$ (d) phosphors [30], irradiated with photons of energy 6.2 eV at 300 K (1) and 77 K (2). At 300 K, intracenter emissions from activators Mn^{2+} (2.06 eV), Dy^{3+} (2.16 and 2.56 eV), and Tb^{3+} (2.5 eV and 2.25 eV) appear in all phosphors. From Figure 2a (curve 2), it is evident that new emission bands emerge after irradiation at 77 K for $Ca_2P_2O_7 - Mn$ at 3.06 eV and 2.92 eV, for $BaSO_4 - Dy$ at 3.1 eV and 2.95 eV, for $Ca_2P_2O_7 - Tb$ at 3.1 eV and 2.95 eV, and for $Ca_3(PO_4)_2 - Mn$ at 3.1 eV and 2.93 eV. It is also noted that at 77 K, the intensity of the intracenter emissions decreases compared to those irradiated at 300 K.

To determine the nature of the new long-wavelength recombination emission bands, their excitation spectra were measured at 77 K for all four phosphors in the spectral range from 3 eV to 6.5 eV.

In Figure 3, it is evident that the excitation spectra for the phosphors $Ca_2P_2O_7 - Mn$ (a) for the bands at 3.06 eV and 2.92 eV after pre-irradiation of the phosphors are at 6.2 eV both at 300 K and at 77 K. It can be seen that the excitation bands appear within the ranges of 3.94–4.0 eV and 4.5–4.6 eV, as well as in a broad range from 5.5 eV to 6.2 eV. In a similar manner, excitation spectra were measured for new long-wavelength recombination emission bands for the phosphors $BaSO_4 - Dy$ (d), $Ca_3(PO_4)_2 - Mn$ (b), and $Ca_2P_2O_7 - Tb$ (c).
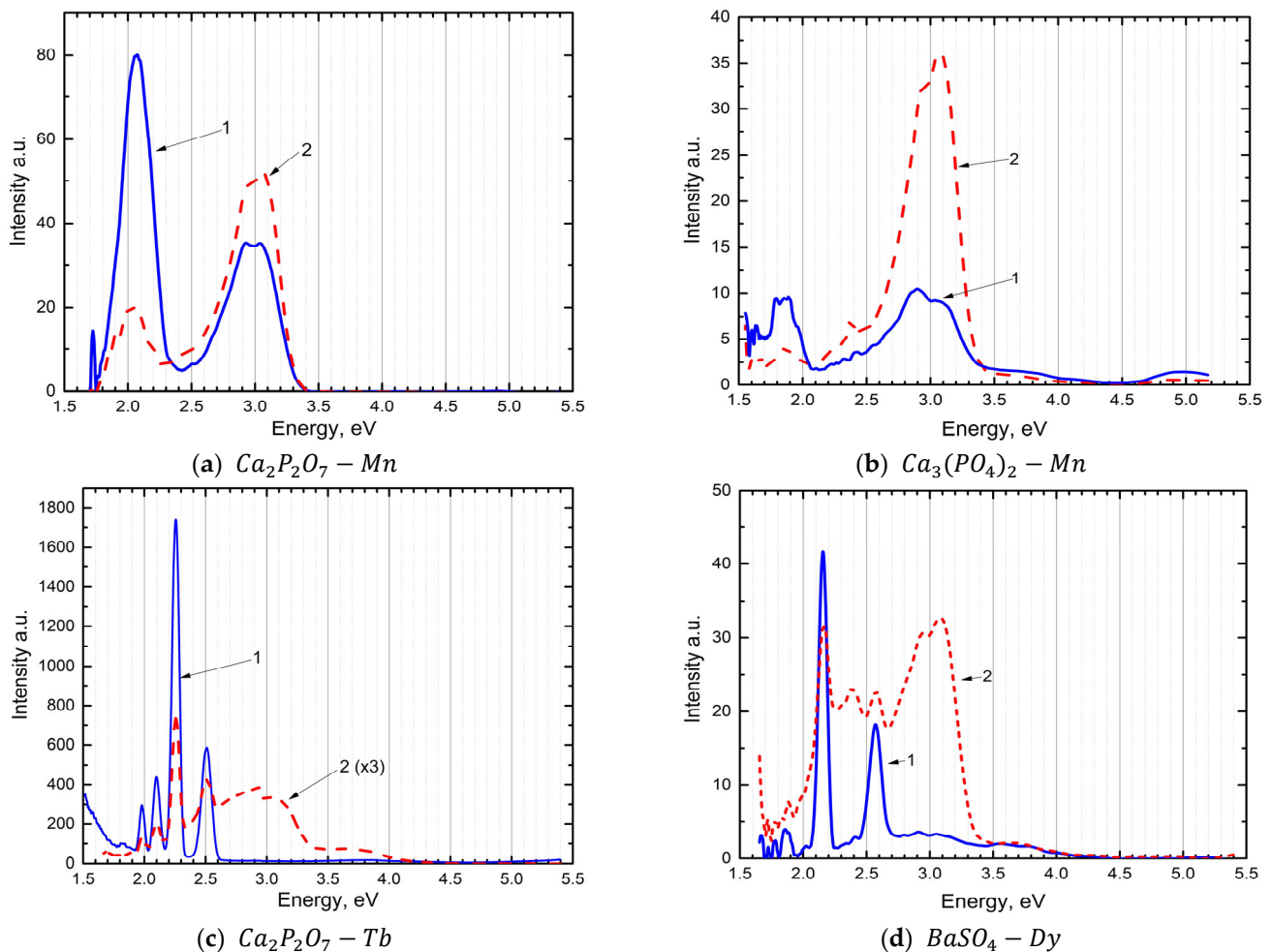
(a) $Ca_2P_2O_7 - Mn$

(b) $Ca_3(PO_4)_2 - Mn$

(c) $Ca_2P_2O_7 - Tb$

(d) $BaSO_4 - Dy$

Figure 2. Emission spectra of phosphors when excited by photons with an energy of 6.2 eV (1—at 300 K; 2—at 77 K).

For 3.1 eV and 2.95 eV at 77 K and 300 K for $BaSO_4 - Dy$.

From Figure 3d, it is evident that these recombination emission bands are excited in the transparency region of the $BaSO_4 - Dy$ matrix at 3.9–4.0 eV and 4.5 eV–4.6 eV at 77 K. Excitation spectra were then measured for new recombination emission bands for the phosphor $Ca_3(PO_4)_2 - Mn$ for the emission band at 2.92 eV at 77 K (1), for 3.06 eV at 77 K (2), and for the band at 3.06 eV at 300 K (3).

Excitation spectra were also measured for recombination emission bands for the band at 3.1 eV at 77 K (1) and for 2.95 eV at 77 K (2) $Ca_2P_2O_7 - Tb$. From Figure 3c, it can be seen that the recombination emission bands are excited in the transparency region of the $Ca_3(PO_4)_2 - Mn$ and $Ca_2P_2O_7 - Tb$ phosphors at 3.9–4.0 eV and 4.5 eV and 4.6 eV at 77 K. In the next stage, excitation spectra were measured for the activator band Mn^{2+}, Tb^{3+}, and Dy^{3+} after pre-irradiation with photons of 6.2 eV energy, which created new recombination emission bands at 3.1 and 2.95 eV, excited in the transparency region of the matrix at 3.95–4.0 eV and 4.5–4.6 eV.

From Figure 4a for $Ca_2P_2O_7 - Mn$, it can be seen that the intracenter emission bands at 2.06 eV for Mn^{2+} were excited by activator excitation at 3.5–3.6 eV. Additionally, Mn^{2+} was excited at 4.0 eV and 4.5 eV, where new recombination emissions at 2.92 eV and 3.06 eV were excited.
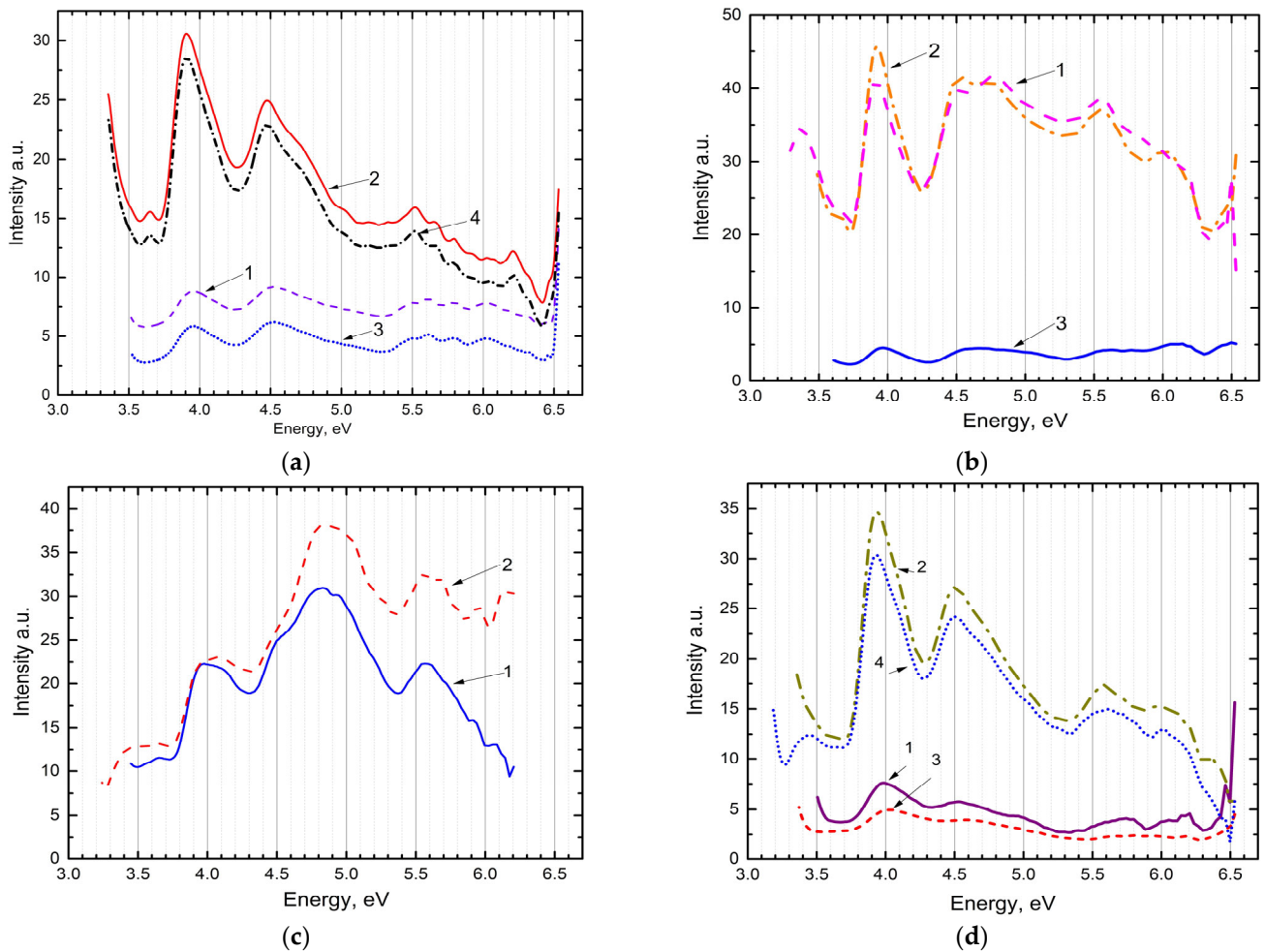
Figure 3. Excitation spectra of pre-irradiated phosphor. $Ca_2P_2O_7 - Mn$ (**a**) 1—for the emission band at 2.92 eV at 300 K; 2—for the emission band at 2.92 eV at 77 K; 3—for the emission band at 3.06 eV at 300 K; 4—for the emission band at 3.06 eV at 77 K. $Ca_3(PO_4)_2 - Mn$ (**b**) 1—for the emission band at 2.92 eV at 77 K; 2—for the emission band at 3.06 eV at 77 K; 3—for the emission band at 3.06 eV at 300 K. $Ca_2P_2O_7 - Tb$ (**c**) 1—for the emission band at 3.1 eV at 77 K; 2—for the emission band at 2.93 eV at 77 K. $BaSO_4 - Dy$ (**d**) for the emission band at 2.95 eV at 300 K (curve 1), at 77 K (curve 2), and for the band at 3.1 eV at 300 K (curve 3) and at 77 K (curve 4).

Also, from Figure 4d, in the measurements of the excitation spectrum of intracenter emission at 2.16 eV and 2.56 eV of $BaSO_4 - Dy$ phosphors after pre-irradiation with photons at 6.2 eV, electron–hole trapping centers were created.

From Figure 4d, it is evident in the excitation spectrum that the activator emissions of Dy^{3+} at 2.56 eV and 2.16 eV are excited at 3.2 eV and 3.40–3.52 eV corresponding to the activator intracenter excitation of Dy^{3+} ion, as well as at 3.9–4.0 eV and 4.5–4.6 eV corresponding to the excitation of long-wavelength recombination emission at 3.1 eV and 2.95 eV.

From Figure 4b for $Ca_3(PO_4)_2 - Mn$ and Figure 4c for $Ca_2P_2O_7 - Tb$, it is visible that the intracenter excitations of Mn^{2+} and Tb^{3+} activators at 77 K are mainly excited in the spectral range of 3.9–4.0 eV and 4.5–4.6 eV, where their intrinsic recombination emissions at 3.06 eV and 2.92 eV for $Ca_3(PO_4)_2 - Mn$ and 3.1 eV and 2.95 eV for $Ca_2P_2O_7 - Tb$ are excited.

It is significant that the activator emissions are excited in the spectral range of 3.9–4.0 eV and 4.5–4.6 eV, where the main recombination emissions at 2.95 eV and 3.1 eV are excited.
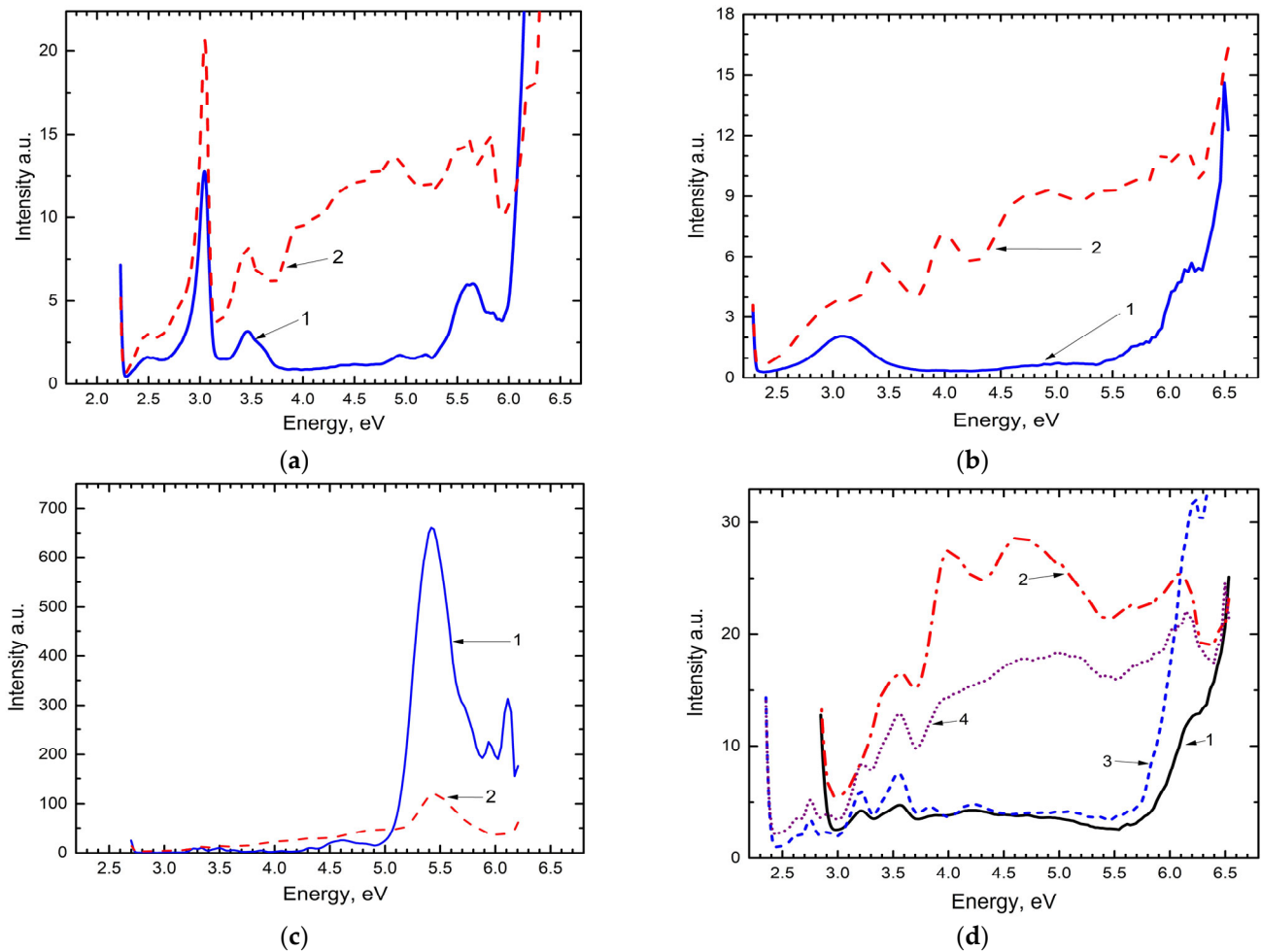
Figure 4. Excitation spectra of intracenter emission. $Ca_2P_2O_7 - Mn$ (**a**) emission for the 2.06 eV band (1—at 300 K; 2—at 77 K). $Ca_3(PO_4)_2 - Mn$ (**b**) emission for the 2.06 eV band (1—at 300 K; 2—at 77 K). $Ca_2P_2O_7 - Tb$ (**c**) for the 2.5 eV emission band (curves 1, 2) at 300 K and 77 K. $BaSO_4 - Dy$ (**d**) for the emission bands at 2.56 eV (curves 1, 2) and 2.16 eV (curves 3, 4) at 77 K and 300 K.

Figure 5 shows the emissions of phosphors $Ca_2P_2O_7 - Mn$ (a), $Ca_3(PO_4)_2 - Mn$ (b), $Ca_2P_2O_7 - Tb$ (c), and $BaSO_4 - Dy$ (d) with induced defects or electron–hole trapping centers when excited by photons with energy of 3.95–4.0 eV (curves 3, 4) and 4.5–4.6 eV (curves 1, 2) at 77 K and 300 K for $BaSO_4 - Dy$. From Figure 5d, it is visible that at 77 K, intense recombination emissions occur at 2.95 eV and 3.1 eV (curve 4, 2) for $BaSO_4$. The experimental results indicate that recombination emissions are indeed excited at photon energies of 3.9–4.0 eV and 4.5–4.6 eV. This implies that the energies corresponding to the emission-producing transitions between the ground and excited local states at 3.1 eV and 2.95 eV are 3.9–4.0 eV and 4.5–4.6 eV, respectively. In Figure 4, we demonstrated that in phosphors with induced defects, recombination emissions at 2.95 eV and 3.1 eV, as well as activator emissions of Dy^{3+}, are excited similarly at these energies of 3.9–4.0 eV and 4.5–4.6 eV. Thus, we presume that upon excitation with 6.2 eV energy, the resulting electron–hole pairs are trapped by SO_4^{2-} anions and Dy^{3+} activators to form $SO_4^{2-} + e^- \rightarrow SO_4^{3-}$ and $Dy^{3+} + e^- \rightarrow Dy^{2+}$, creating electron trapping centers SO_4^{3-} and Dy^{2+}. These electron centers are complementary to localized SO_4^- holes above the valence band, forming intrinsic and activator trapping centers $SO_4^{3-} - SO_4^-$ and $Dy^{2+} - SO_4^-$ spaced apart by energies of 3.9–4.0 eV and 4.5–4.6 eV in the transparency region of the phosphor matrix.

In Figure 5a–c, similar experimental data were obtained for the phosphors $Ca_2P_2O_7 - Mn$, $Ca_3(PO_4)_2 - Mn$ and $Ca_2P_2O_7 - Tb$.
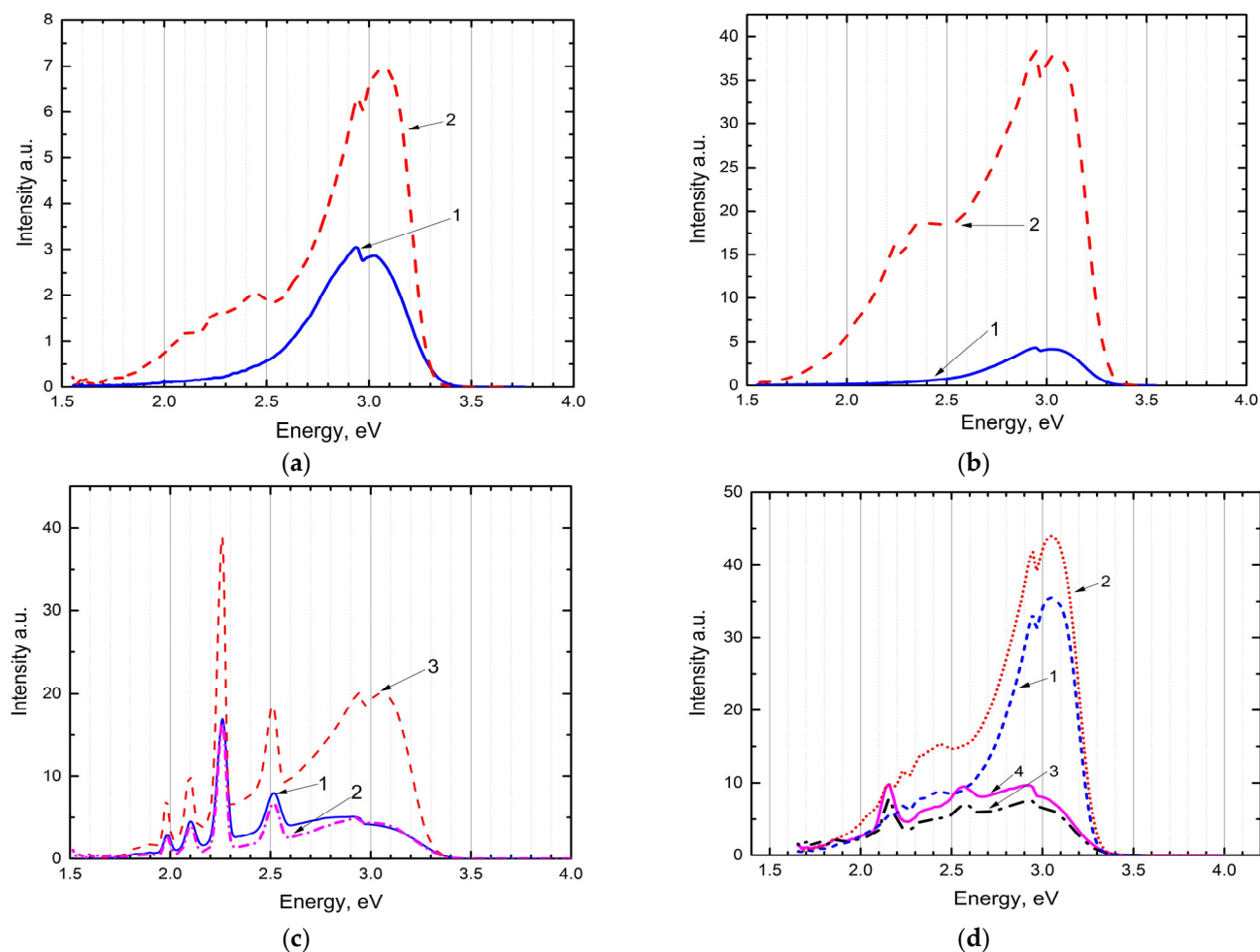
Figure 5. Emission spectra of the phosphor. $Ca_2P_2O_7 - Mn$ (**a**) when excited by photons with energies of 3.95–4.0 eV at 300 K and 77 K (curves 1, 2). $Ca_3(PO_4)_2 - Mn$ (**b**) when excited by photons with an energy of 3.9–4.0 eV at 300 K (curves 1) and 77 K (curves 2). $Ca_2P_2O_7 - Tb$ (**c**) when excited by photons with an energy of 3.9 eV: 1—at 300 K; 3—at 77 K; and 4.4 eV: 2—at 300 K. $BaSO_4 - Dy$ (**d**) when excited by photons with an energy of 3.95–4.0 eV (curves 3, 4) and 4.5–4.6 eV at 300 K and 77 K, respectively (curves 1, 2).

When these phosphors with induced trapping centers are excited by photons with energies of 4.0 eV and 4.5 eV, recombination emissions occur at 3.1 eV and 2.95 eV. We demonstrated these recombination emissions in Figure 3, excited by photon energies of 4.0 and 4.5 eV. Figure 4a–d show that intracenter emissions from activators Mn^{2+}, Dy^{3+}, and Tb^{3+} are also excited by photon energies of 4.0 eV and 4.5 eV. Thus, experimental evidence shows that intrinsic recombination emissions at ~3.1 eV and ~2.95 eV are excited simultaneously with activator emissions from Mn^{2+}, Dy^{3+}, and Tb^{3+} at photon energies of 4.0 eV and 4.5 eV.

Figure 6a shows the excitation spectrum of the emission of $Ca_2P_2O_7 - Mn$ for the bands at 2.0 eV and 2.1 eV at 300 K and 15 K. Figure 6a demonstrates that the emission of Mn^{2+} is excited at photon energies of 7.85 eV, which represents the bandgap of the $Ca_2P_2O_7 - Mn$ phosphor.

To conclusively determine the nature of the new recombination luminescent states at 2.92–2.95 eV and 3.1–3.15 eV, which are excited in the transparency region of the phosphor matrix at 3.9–4.0 eV and 4.5–4.6 eV, their excitation spectra were investigated in the vacuum ultraviolet region from 4 eV to 12 eV at temperatures from 15 K to 300 K.
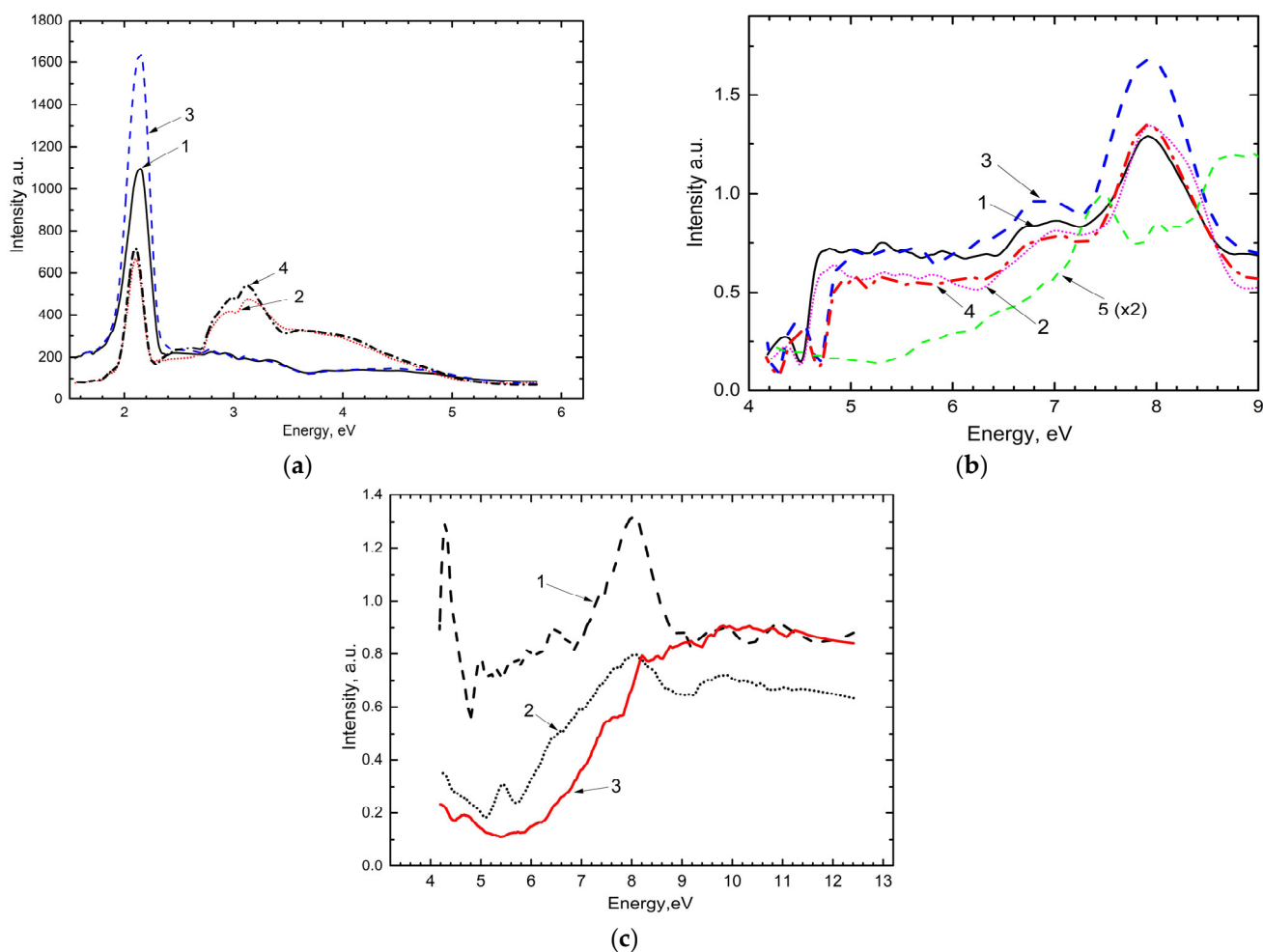
Figure 6. Emission and excitation spectra of the samples. $Ca_2P_2O_7$ (**a**) phosphor when excited by photons of 8.26 eV (1—at 300 K; 2—at 15 K) and when excited by photons of 7.75 eV (3—at 300 K; 4—at 15 K). $Ca_2P_2O_7 - Mn$ (**b**) for the emission band at 2.0 eV: 1—at 300 K; 2—at 15 K; for the emission band at 2.1 eV: 3—at 300 K; 4—at 15 K; and for the emission band at 2.95 eV: 5—at 15 K. $BaSO_4 - Dy$ (**c**) in the VUV region for emission bands: 1—2.16 eV; 2—2.56 eV; 3—3.1 eV.

Figure 6c presents the excitation spectrum of the intracenter emission at 2.56 eV and 2.16 eV at 15 K in the $BaSO_4 - Dy$ (c) powder. From the figure, it is evident that the intracenter emissions at 2.56 eV and 2.16 eV are excited at photon energies around 8 eV. According to the authors' [33] hypothesis, in the spectral region of 8–8.4 eV, it corresponds to the excitation of the anionic complex SO_4^{2-} in rare-earth metal sulfates. These values correspond to the bandgap of alkaline earth metal sulfates.

From Figure 6a, it is evident that when the phosphor $Ca_2P_2O_7 - Mn$ is excited with photon energies of 8.26 eV and 7.75 eV at 300 K, intracenter emissions of the Mn^{2+} ion are observed (curves 1 and 3). At a reduced temperature of 15 K, the intensity of the 2.06 eV emission decreases by 2–2.5 times, and new emission bands at 2.92 eV and 3.06 eV appear (curves 2 and 4, Figure 6a). This pattern of emission is consistent with observations made during UV irradiation with a photon energy of 6.2 eV at 77 K for the phosphor $Ca_2P_2O_7 - Mn$.

Intracenter excitation of Dy^{3+} ions in the phosphor $BaSO_4 - Dy$ at these photon energies indicates the creation of electron–hole pairs upon excitation of the anionic complex.

A key finding from these experiments is the excitation of new recombination emissions at 3.1 eV in the phosphors $Ca_2P_2O_7 - Mn$ and $BaSO_4 - Dy$ (Figure 6b,c), in the energy spectral interval from 6 eV to 9 eV. The experimental result indicates that in these phosphors,

upon excitation with photons from 5.5 to 6 eV, electron transfer occurs from the excited anion $SO_4^{2-} - (P_2O_7)^{4-}$ to Dy^{3+} and the neighboring ion SO_4^{2-}, resulting in charge transfer from oxygen $\left(O^{2-} - Dy^{3+}\right)$ to the activators $\left(O^{2-} - SO_4^{2-}\right)$ to the neighboring ion, creating electron trapping centers Dy^{2+}, SO_4^{3-}, Mn^+, and $(P_2O_7)^{3-}$. The efficiency of electron trapping centers Dy^{2+} and SO_4^{3-} gradually increases up to the creation of free electron–hole pairs at 8.4–9 eV, in the phosphors $Ca_2P_2O_7 - Mn$ and $BaSO_4 - Dy$ (Figure 6a–c curve 3).

In the next phase, the temperature dependence of the recombination emissions at 3.1 and 2.95 eV and the activator emissions Mn^{2+}, Dy^{3+}, and Tb^{3+} were measured in four phosphors.

By measuring the temperature dependence of recombination emissions at 3.1 eV and 2.95 eV in $BaSO_4 - Dy$, it can be demonstrated that their decay is associated with intrinsic recombination emission (Figure 7d) occurring in the system $SO_4^{-3}—SO_4^{-}$, as well as with the restored activator emissions related to the decay of $Dy^{2+}—SO_4^{-}$: $Dy^{2+} \rightarrow Dy^{3+} + e^-$; $e^- + SO_4^{-} \rightarrow hv$. From Figure 7d, it is visible that the recombination emissions at 3.1 eV and 2.95 eV radiatively decay in the temperature intervals of 150–200 K and 250–300 K (curves 1 and 2).
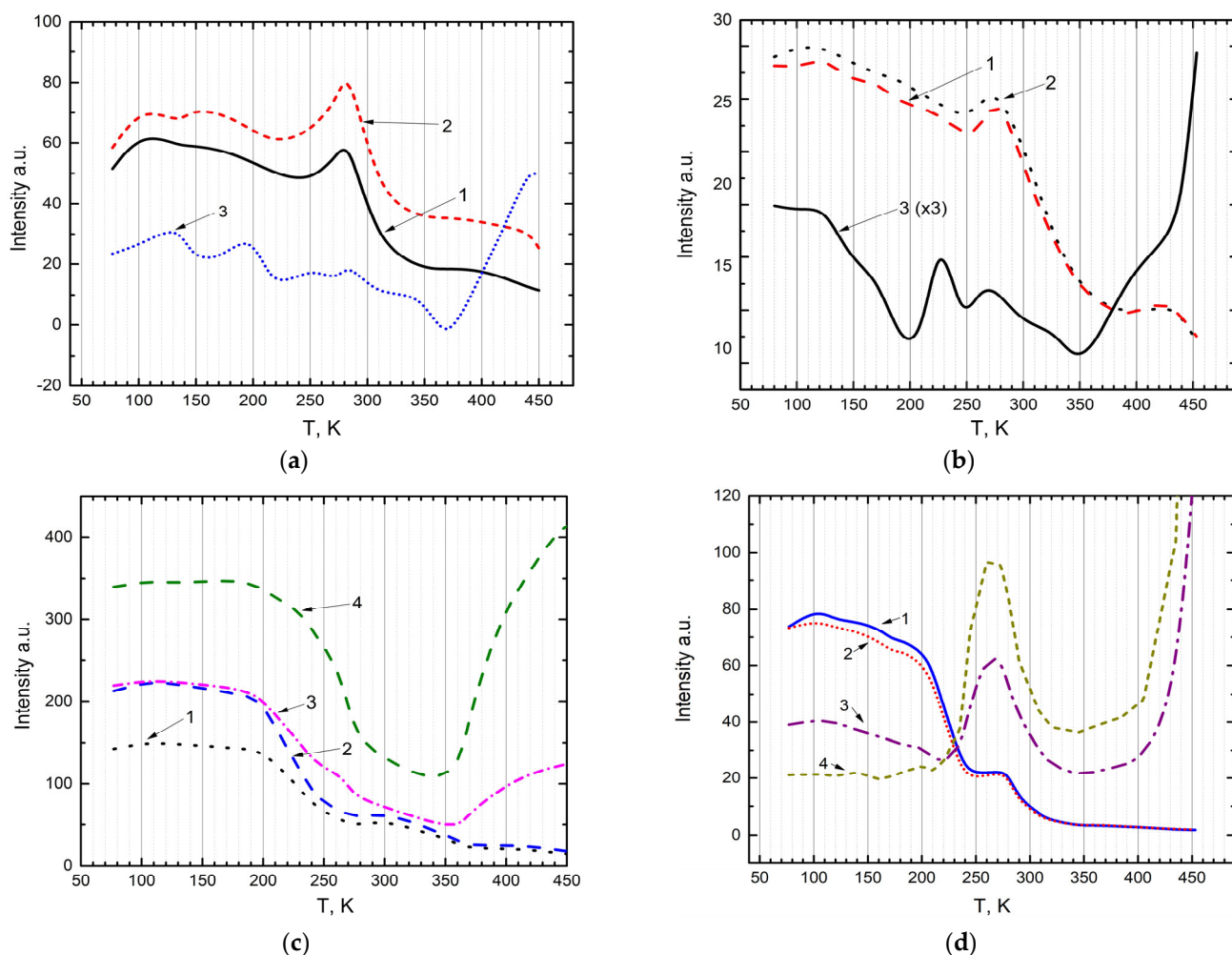

Figure 7. Temperature dependence of the emission. $Ca_2P_2O_7 - Mn$ (**a**): 1—at 2.95 eV; 2—at 3.1 eV; 3—at 2.06 eV. $Ca_3(PO_4)_2 - Mn$ (**b**): 1—at 2.95 eV; 2—at 3.1 eV; 3—at 2.06 eV (curve 3, magnified three times). $Ca_2P_2O_7 - Tb$ (**c**) for the emission bands: (1) 3.1 eV; (2) 2.92 eV; (3) 2.51 eV; (4) 2.25 eV. $BaSO_4 - Dy$ (**d**) for the emission bands: (1) 3.1 eV; (2) 2.95 eV; (3) 2.56 eV; (4) 2.16 eV.

Emission of Dy^{3+} is asymmetrically restored in these processes (curve 3) in the temperature range of 200–205 K and 330 K–370 K during the ionization of $Dy^{2+} \rightarrow Dy^{3+} + e^-$, restoring the Dy^{3+} ion and increasing its concentration (Figure 7d, curve 3). The ionized

e^- recombines with the SO_4^- hole, emitting hv, which is transferred to the Dy^{3+} activators, and the emission at 2.16 eV is observed.

Figure 7d shows that the recombination emissions at 3.1 eV and 2.95 eV, in the temperature range of 200–300 K, which quickly decay radiatively in $BaSO_4 - Dy$ (Figure 7d, curves 1,2). The same figure also shows the temperature dependence of intracenter emission of Dy^{3+} at 2.56 eV and 2.16 eV: from 100 K to 200 K, the intensity remains unchanged, but in the range of 230–300 K, the emissions of Dy^{3+} intensify, because in this temperature range the activator electronic states of Dy^{2+} decay. Thus, for $Dy^{2+} \rightarrow Dy^{3+} + e^-$, the electron recombines with a hole localized above the valence band near the Dy^{3+} activator, transferring the energy of the recombination process to the Dy^{3+} activator, resulting in the intensification of Dy^{3+} emission.

Further increases in temperature lead to an increase in the intensity of Dy^{3+} emission.

A similar temperature dependence is shown in Figure 7a. Similar energy transfer processes occur from the matrix to the emitter Mn^{2+}. During irradiation, a combined electron-emitting state consisting of intrinsic and activator trapping centers $Mn^+ - (P_2O_7)^{3-}$ and $(P_2O_7)^{5-} - (P_2O_7)^{3-}$ forms, from whose decay recombination emissions at 3.1 eV and 2.95 eV arise (curves 1 and 2 in Figure 7a). In the temperature range of 250–350 K, these emissions decay radiatively in a similar mechanism as shown in Figure 7d, flaring up in the temperature range of 250–300 K and then decreasing to a minimum value.

The activator electronic components of the combined state $Mn^+ - (P_2O_7)^{3-}$ decay in a similar manner $Mn^+ \rightarrow Mn^{2+} + e^-$, and the electron recombines with the hole $(P_2O_7)^{3-} \rightarrow hv$. Above the temperature of 370 K, the ionization of $Mn^+ \rightarrow Mn^{2+} + e^-$ is observed, transferring the energy of the recombination process to Mn^{2+}. In the range of 370–450 K, an increase in the intensity of Mn^{2+} emission is observed. In the other two phosphates, the temperature dependence of the decay of combined states and the restoration of activator emissions during their ionization occur similarly (Figure 7b,c).

Figure 8 shows a model of the energy state of trapping centers in the band diagram. The diagram illustrates the upper part of the valence band and the conduction band. The left side of the figure shows the formation of electron–hole trapping centers. Electrons created are trapped by activators $Dy^{3+} + e^- \rightarrow Dy^{2+}$, forming electron trapping centers (Figure 8a). The hole SO_4^- is trapped by the ground state of Dy^{3+} located above the valence band. The middle part shows a schematic of the fundamental and low-energy excited states of the Dy^{3+} activator.

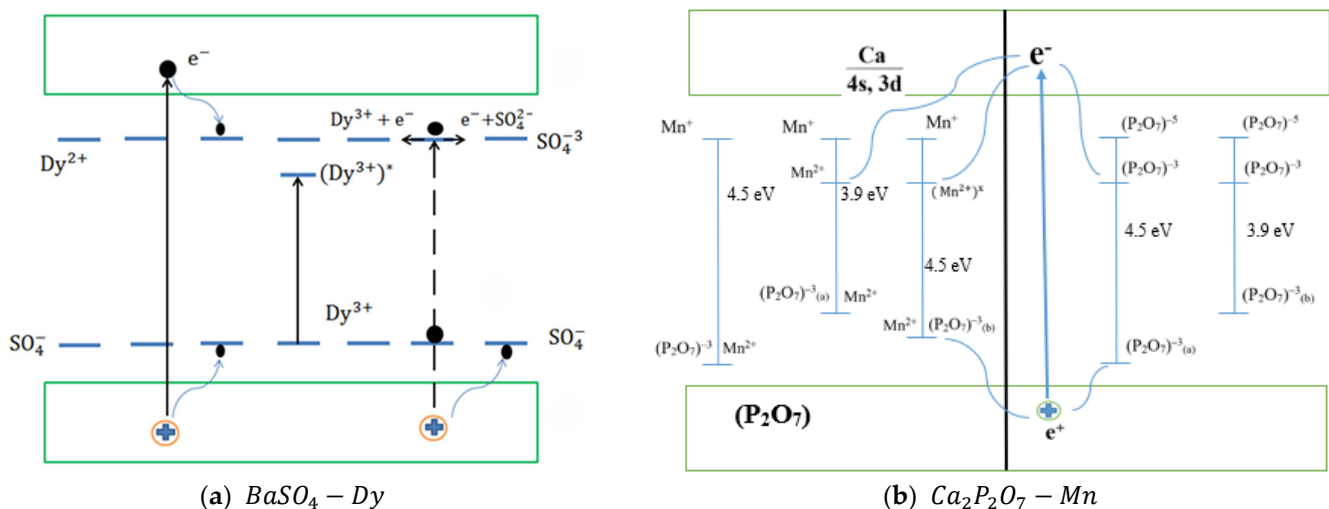(a) $BaSO_4 - Dy$ (b) $Ca_2P_2O_7 - Mn$

Figure 8. Band diagram of electron–hole trapping centers.

The left part of the diagram shows the charge transfer from the excited state of the anion SO_4^{2-} to the Dy^{3+} ion and the neighboring anion $SO_4^{2-} + e^-$. This results in the formation of the electron trapping center Dy^{2+} and SO_4^{3-} by the reactions $Dy^{3+} + e^- \rightarrow Dy^{2+}$ and $SO_4^{2-} + e^- \rightarrow SO_4^{3-}$.

Figure 8b is a similar band diagram model for $Ca_2P_2O_7 - Mn$.

In this work, we investigated the mechanism of energy transfer from intrinsic electronic excitations to activators in the phosphors $Ca_2P_2O_7 - Mn$, $BaSO_4 - Dy$, $Ca_2P_2O_7$—Tb, and $Ca_3(PO_4)_2 - Mn$.

5. Discussion

Based on the obtained experimental data, the mechanism of energy transfer of electronic excitations, arising during external irradiation in oxyanion phosphors, to emitters, i.e., activators, is discussed. The process of energy transfer from the matrix to the emitters occurs in stages: first, the energy from external irradiation must be accumulated in the phosphors. In our previous works [34], the accumulation of electronic excitation energy in the form of the formation of intrinsic and activator trapping centers, such as $SO_4^{3-} - SO_4^-$ and $Mn^+ - SO_4^-$, was studied in irradiated $CaSO_4 - Mn$ and $BaSO_4 - Mn$ phosphors.

It was proposed that trapping centers are formed under irradiation with photons whose energy exceeds the bandgap, leading to the creation of electron–hole pairs. The generated electrons are trapped by anionic complexes SO_4^{2-} and activators Mn^{2+}, while the holes are localized in the form of the SO_4^- radical above the valence band.

In this study, we demonstrated in several phosphors that the accumulation of electronic excitation energy resulting from external irradiation is stored in the form of new formations—combined electronic-emission states. These combined electronic-emission states consist of both intrinsic and activator electron–hole trapping centers. The formation of combined electronic-emission states and their decay through recombination emissions occur as stepwise processes.

We experimentally demonstrated that under photon irradiation with energies of 5.9–6.2 eV at room temperature, activator emissions were observed in phosphors such as $Ca_2P_2O_7 - Mn$, $BaSO_4 - Dy$, $Ca_2P_2O_7 - Tb$, and $Ca_3(PO_4)_2 - Mn$. The emissions were detected at 2.06 eV for Mn^{2+}, 2.16 and 2.56 eV for Dy^{3+}, and 2.5 and 2.25 eV for Tb^{3+}. At low temperatures (15–77 K), new recombination emissions appeared in all four irradiated phosphors in the spectral ranges of 2.91–2.95 eV and 3.1–3.15 eV with high efficiency.

Measurements of the excitation spectra of these new formations in the spectral intervals of 2.91–2.95 eV and 3.1–3.15 eV in all four phosphors revealed that these recombination emissions are excited by photons with energies of 3.9–4.0 eV and 4.5–4.6 eV. As a result, localized electronic and hole states separated by 3.9–4.0 eV and 4.5–4.6 eV were observed within the transparency region of the matrix. When these phosphors with trapping centers were excited by photons with energies of 3.9–4.0 eV and 4.5–4.6 eV at low temperatures, emissions of combined states at 2.91–2.95 eV and 3.1–3.15 eV were observed. These energies (3.9–4.0 eV and 4.5–4.6 eV) correspond to the excitation spectra of the combined electronic-emission states.

Based on experimental results, it is proposed that in the irradiated sulfates and phosphates $Ca_2P_2O_7 - Mn$, $BaSO_4 - Dy$, $Ca_2P_2O_7 - Tb$, and $Ca_3(PO_4)_2 - Mn$, intrinsic and activator electron trapping centers are formed, such as $SO_4^{3-} - SO_4^-$, $Dy^{2+} - SO_4^-$, $(P_2O_7)^{5-} - (P_2O_7)^{3-}$, $Mn^+ - (P_2O_7)^{3-}$, $Tb^{2+} - (P_2O_7)^{3-}$, $(PO_4)^{5-} - (PO_4)^{3-}$, and $Mn^+ - (PO_4)^{3-}$.

The intrinsic and activator trapping centers are formed through the localization of electrons on intrinsic anions $(P_2O_7)^{4-}$, $(PO_4)^{3-}$ and SO_4^{2-} and on activators Mn^{2+}, Dy^{3+}, and Tb^{3+}, according to the following reactions: $(P_2O_7)^{4-} + e^- \rightarrow (P_2O_7)^{5-}$,

$(PO_4)^{3-} + e^- \rightarrow (PO_4)^{4-}$, $SO_4^{2-} + e^- \rightarrow SO_4^{3-}$, $Mn^{2+} + e^- \rightarrow Mn^+$, $Dy^{3+} + e^- \rightarrow Dy^{2+}$, and $Tb^{3+} + e^- \rightarrow Tb^{2+}$. It was experimentally shown that the intrinsic trapping centers $(P_2O_7)^{5-} - (P_2O_7)^{3-}$, $(PO_4)^{4-} - (PO_4)^{3-}$, and $SO_4^{3-} - SO_4^-$ and the activator centers $Mn^+ - (P_2O_7)^{3-}$, $Mn^+ - (PO_4)^{3-}$, $Tb^{3+} - (P_2O_7)^{3-}$, and $Dy^{3+} - (P_2O_7)^{3-}$ are localized within the transparency region of the matrix and are excited by photons with energies of 3.9–4.0 eV and 4.5–4.6 eV.

Measurements of the excitation spectrum of activator emissions and emissions from combined states in the vacuum ultraviolet region of the spectrum revealed that the excitation spectrum of activator emissions corresponds to the bandgap of the phosphors, where electron–hole pairs in the matrix are generated. The excitation spectrum of combined emission at 3.1 eV showed that emissions are generated in the spectral range from 4.4 eV to 7.8 eV as a result of charge transfer from excited anions to activators and intrinsic anions. Beyond this energy range (7.8–10 eV), combined electronic-emission states are formed due to the trapping of free electrons by activators and anions.

The study of the creation spectrum for combined electronic-emission states at 3.1 eV over a wide spectral range demonstrated that in the photon energy region from 4.4 eV to 6.2 eV, the efficiency of forming electron trapping centers is an order of magnitude lower than in the vacuum ultraviolet region (7.8–10 eV), where free electron–hole pairs are generated. The experimental results confirm that the formation of activator electron trapping centers such as Mn^+ and Dy^{2+} constitutes a structural component of the combined electronic-emission states.

One of the key findings is the excitation of all activators in the phosphors with trapping centers at photon energies of 3.9–4.0 eV and 4.5–4.6 eV, where combined electronic-emission states are excited. This indicates that activators such as Mn^{2+}, Tb^{3+}, and Dy^{3+} in phosphate and sulfate matrices are excited through intracenter absorption within the matrix and also contribute to the excitation spectra of localized combined emission states, which differ in intracenter excitation energies. Thus, activators are excited within the combined emission states (4.0 eV and 4.5 eV).

The temperature dependence measurements of combined states showed that in the temperature range of 200 K to 350 K, the intensity of recombination emissions at 2.92–2.95 eV and 3.06–3.15 eV decreases to a minimum, while activator emissions from Mn^{2+}, Tb^{3+}, and Dy^{3+} are restored, significantly increasing in intensity.

It is suggested that the increase in activator emission intensity is associated with the restoration of the charge states during ionization of the electron trapping centers, according to the following reactions: $Mn^+ - e^- \rightarrow Mn^{2+}$, $Tb^{2+} - e^- \rightarrow Tb^{3+}$, and $Dy^{2+} - e^- \rightarrow Dy^{3+}$.

Electrons ionized from activator electron trapping centers recombine with holes localized near the activators, and the energy generated in this process is transferred to the activators. The excited activators emit corresponding intracenter emissions.

Thus, it is proposed that in combined states, the energy of intrinsic matrix excitation accumulates, and during the decay process, the energy released in the matrix recombination process is transferred to the activators.

6. Conclusions

In all phosphors, combined electronic-emission states are formed from the electronic-emission states of intrinsic and activator trapping centers during ultraviolet excitation with photon energies of 6.2–10 eV at temperatures of 15–77 K.

Measurements of the excitation spectra for combined emission states at 3.06–3.1 eV and 2.92–2.95 eV, as well as activator emissions from Mn^{2+}, Tb^{3+}, and Dy^{3+} in the four

irradiated phosphors, showed that they are simultaneously excited by photon energies of 3.9–4.0 eV and 4.5–4.6 eV.

Photon energies of 3.9–4.0 eV and 4.5–4.6 eV, which simultaneously excite intrinsic recombination emissions at 3.06–3.1 eV and 2.92–2.95 eV, constitute the excitation spectra of the combined states in the phosphors.

Thermal excitation of all phosphors up to 250–300 K leads to the decay of the new combined emission states due to the ionization of intrinsic and activator electron trapping centers. The energy generated during the recombination of electrons, formed through ionization, with holes localized in the ground state of activators, is transferred to the emitters.

Author Contributions: Conceptualization, A.K., A.Z. and S.P.; Methodology, A.K., A.Z. and S.P.; Investigation, A.S.N. and T.T.A.; Writing–original draft, T.N.; Writing–review & editing, A.S.N., T.T.A. and T.N.; Visualization, A.S.N. and T.T.A.; Supervision, T.N. All authors have read and agreed to the published version of the manuscript.

Data Availability Statement: The original contributions presented in the study are included in the article material, further inquiries can be directed to the corresponding authors.

Conflicts of Interest: The authors declare that there is no conflict of interest.

References

1. Zhou, R.; Lin, L.; Liu, C.; Dorenbos, P.; Tao, Y.; Huang, Y.; Liang, H. Insight into Eu redox and Pr^{3+} 5d emission in $KSrPO_4$ by VRBE scheme construction. *Dalton Trans.* **2018**, *47*, 306–313. [CrossRef] [PubMed]
2. Griesiute, D.; Garskaite, E.; Antuzevics, A.; Klimavicius, V.; Balevicius, V.; Zarkov, A.; Katelnikovas, A.; Sandberg, D.; Kareiva, A. Synthesis, structural and luminescent properties of Mn-doped calcium pyrophosphate ($Ca_2P_2O_7$) polymorphs. *Sci. Rep.* **2022**, *12*, 7116. [CrossRef] [PubMed]
3. Lecointre, A.; Bessière, A.; Bos, A.J.J.; Dorenbos, P.; Viana, B.; Jacquart, S. Red long-lasting phosphorescence (LLP) in *β-TCP* type $Ca_{9.5}Mn (PO_4)_7$ compounds. *Opt. Mater.* **2011**, *34*, 376–380. [CrossRef]
4. Sinusaite, L.; Antuzevics, A.; Popov, A.I.; Rogulis, U.; Misevicius, M.; Katelnikovas, A.; Kareiva, A.; Zarkov, A. Synthesis and luminescent properties of *Mn*-doped alpha-tricalcium phosphate. *Ceram. Int.* **2021**, *47*, 5335–5340. [CrossRef]
5. Cao, R.; Wang, W.; Zhang, J.; Ye, Y.; Chen, T.; Guo, S.; Xiao, F.; Luo, Z. Luminescence properties of $Sr_2Mg_3P_4O_{15}$:Mn^{2+} phosphor and the improvement by co-doping Bi^{3+}. *Opt. Mater.* **2018**, *79*, 223–226. [CrossRef]
6. Morgan, M.D.; Stoebe, T.G. Optical absorption and luminescent processes in thermoluminescent $CaSO_4$:Dy. *J. Phys. Condens. Matter* **1989**, *1*, 5773–5781. [CrossRef]
7. Matthews, R.J.; Stoebe, T.G. Thermoluminescent spectra and optical absorption in $CaSO_4$:Dy. *J. Phys. C Solid State Phys.* **1982**, *15*, 6271–6280. [CrossRef]
8. Danby, R.J.; Boas, J.F.; Calvert, R.L.; Pilbrow, J.R. ESR of thermoluminescent centres in $CaSO_4$ single crystals. *J. Phys. C Solid State Phys.* **1982**, *15*, 2483–2493. [CrossRef]
9. Morgan, M.D.; Stoebe, T.G. An electron spin resonance study of thermoluminescence mechanisms in $CaSO_4$:Dy. *J. Phys. Condens. Matter* **1990**, *2*, 1619–1634. [CrossRef]
10. Barkyoumb, J.; Mathur, V.; Lewandowski, A.; Tookey, A.; Townsend, P.; Giblin, I. Low-temperature luminescence properties of $CaSO_4$:Dy. *J. Lumin.* **1997**, *72–74*, 629–632. [CrossRef]
11. Zhai, B.-G.; Liu, D.; He, Y.; Yang, L.; Huang, Y.M. Tuning the photoluminescence of Eu^{2+} and Eu^{3+} co-doped $SrSO_4$ through post annealing technique. *J. Lumin.* **2018**, *194*, 485–493. [CrossRef]
12. Sharma, K.; Bahl, S.; Singh, B.; Kumar, P.; Lochab, S.; Pandey, A. $BaSO_4$:Eu as an energy independent thermoluminescent radiation dosimeter for gamma rays and C^{6+} ion beam. *Radiat. Phys. Chem.* **2018**, *145*, 64–73. [CrossRef]
13. Tang, Q.; Tang, H.; Luo, D.; Zhang, C.; Guo, J.; Wu, H. Thermoluminescence spectra and dose responses of $SrSO_4$ phosphors doped with rare earths (Eu, Dy, Tm) and phosphorus. *Radiat. Prot. Dosim.* **2019**, *187*, 164–173. [CrossRef] [PubMed]
14. Jamkhaneh, K.B.; Saraee, K.R.E. Thermoluminescence characterization of nanocrystalline powder of $SrSO_4$:Sm exposed to gamma radiation for dosimetric applications. *Appl. Radiat. Isot.* **2020**, *160*, 109128. [CrossRef]

15. Kumar, M.; Nagabhushana, H.; Ratnakaram, Y. Influence of alkali and alkaline earths on structural and luminescence properties of Sm^{3+} doped lithium fluoro phosphate glass and different (Na, Mg, K, Ca and Sr) glass ceramics. *J. Non-Cryst. Solids* **2021**, *573*, 121146. [CrossRef]

16. Okada, G.; Hirasawa, K.; Kusano, E.; Yanagida, T.; Nanto, H. Radio-photoluminescence properties of samarium-doped alkaline earth sulfates. *Nucl. Instrum. Methods Phys. Res. Sect. B Beam Interact. Mater. Atoms* **2020**, *466*, 56–60. [CrossRef]

17. Suresh, S.; Rita, A.; Dhas, S.A.M.B.; Rao, R.G.S.; Biju, C.S. Effect of annealing on the photoluminescence and thermoluminescence properties of Eu^{2+} doped $BaSO_4$ microgravels. *J. Mater. Sci. Mater. Electron.* **2020**, *31*, 11113–11122. [CrossRef]

18. Rani, R.S.; Lakshmanan, A. The role of anion and cation vacancies in the thermoluminescence and photoluminescence processes of $BaSO4:Eu^{2+}$. *J. Lumin.* **2016**, *174*, 63–69. [CrossRef]

19. Cao, R.; Qin, Z.; Yu, X.; Wu, D.; Zheng, G.; Li, W. Synthesis and luminescence properties of $BaSO_4$ phosphor activated with Sm. *Optik* **2016**, *127*, 1126–1129. [CrossRef]

20. Saraee, K.R.E.; Kharieky, A.A.; Khosravi, M.; Abdi, M.R.; Zeinali, H.Z. Themoluminescence properties of nanocrystalline of $BaSO_4:Dy,Tb$ irradiated with gamma rays. *J. Lumin.* **2013**, *137*, 230–236. [CrossRef]

21. Omanwar, S.K.; Palan, C.B. Synthesis and preliminary OSL studies of Ce^{3+} activated calcium sulfate ($CaSO_4$) for radiation dosimetry. *J. Mater. Sci. Mater. Electron.* **2018**, *29*, 7388–7392. [CrossRef]

22. Yüksel, M.; Dogan, T.; Portakal, Z.G.; Topaksu, M. Synthesis and luminescence characterization of microcrystalline Nd-doped calcium sulfate. *Appl. Radiat. Isot.* **2019**, *148*, 197–203. [CrossRef] [PubMed]

23. Manam, J.; Das, S. Determination of kinetic parameters of thermally stimulated luminescence of Cu-doped $BaSO_4$. *J. Phys. Chem. Solids* **2009**, *70*, 379–384. [CrossRef]

24. Annalakshmi, O.; Jose, M.T.; Madhusoodanan, U. Synthesis and characterisation of $BaSo_4:Eu$ thermoluminescence phosphor. *Radiat. Prot. Dosim.* **2012**, *150*, 127–133. [CrossRef]

25. Azorin, J. Preparation methods of thermoluminescent materials for dosimetric applications: An overview. *Appl. Radiat. Isot.* **2014**, *83*, 187–191. [CrossRef]

26. Bhoyar, P.D.; Dhoble, S. Study of electron vibrational interaction parameters in chlorophosphate activated with Eu^{2+} ion. *Mater. Chem. Phys.* **2014**, *147*, 488–491. [CrossRef]

27. Cano, N.F.; Rao, T.G.; Silva-Carrera, B.N.; Cruz, S.P.; Javier-Ccallata, H.S.; Bedoya-Barriga, Y.A.; Ayala-Arenas, J.S.; Watanabe, S. Elucidation of the centers responsible for the TL peaks in the anhydride crystal. *J. Lumin.* **2020**, *221*, 117082. [CrossRef]

28. Okada, G.; Koguchi, Y.; Yanagida, T.; Nanto, H. Undoped $CaSO_4$ showing highly enhanced radio-photoluminescence properties. *Mater. Today Commun.* **2020**, *24*, 101013. [CrossRef]

29. Nurakhmetov, T.N.; Alibay, T.T.; Zhangylyssov, K.B.; Daurenbekov, D.H.; Salikhodzha, Z.M.; Shamiyeva, R.K.; Sadykova, B.M.; Yussupbekova, B.N.; Tolekov, D.A. Energy Transfer in the $CaSO_4$−Dy Thermoluminescent Dosimeter from the Excited State of the $SO_4{}^{2-}$ Anionic Complex to the Activators. *Crystals* **2023**, *13*, 1596. [CrossRef]

30. Nurakhmetov, T.; Zhangylyssov, K.; Shamiyeva, R.; Alibay, T.; Salikhodzha, Z.; Sadykova, B.; Tolekov, D.; Yussupbekova, B. The energy transfer of electronic excitations to impurities in dosimetric phosphors $BaSO_4$-Dy. *NIMP B* **2024**, *555*, 165459. [CrossRef]

31. Nurakhmetov, T.N.; Alibay, T.T.; Zhangylyssov, K.B.; Nurpeissov, A.S.; Pazylbek, S.; Griesiute, D.; Zarkov, A.; Kareiva, A. Luminescence and Electron–Hole-Trapping Centers in α-$Ca_2P_2O_{7\_}Mn$. *Crystals* **2024**, *14*, 406. [CrossRef]

32. Döbelin, N.; Maazouz, Y.; Heuberger, R.; Bohner, M.; Armstrong, A.A.; Johnson, A.J.W.; Wanner, C. A thermodynamic approach to surface modification of calcium phosphate implants by phosphate evaporation and condensation. *J. Eur. Ceram. Soc.* **2020**, *40*, 6095–6106. [CrossRef]

33. Dorenbos, P. The 5d level positions of the trivalent lanthanides in inorganic compounds. *J. Lumin.* **2000**, *91*, 155–176. [CrossRef]

34. Nurakhmetov, T.N.; Alibay, T.T.; Zhangylyssov, K.B.; Daurenbekov, D.H.; Zhunusbekov, A.M.; Kainarbay, A.Z.; Sadykova, B.M.; Tolekov, D.A.; Shamiyeva, R.K. Specific Features of Formation of Electron and Hole Trapping Centers in Irradiated $CaSO_4$-Mn and $BaSO_4$-Mn. *Crystals* **2023**, *13*, 1054. [CrossRef]